

Surface electronic structures of the Eu-induced Si(111)-(3×2) and -(2×1) reconstructions

Kazuyuki Sakamoto,^{1,*} A. Pick,² and R. I. G. Uhrberg²

¹*Department of Physics, Graduate School of Science, Tohoku University, Sendai, 980-8578, Japan*

²*Department of Physics and Measurement Technology, Linköping University, S-581 83 Linköping, Sweden*

(Received 12 January 2005; published 7 July 2005)

The electronic structures of the Eu/Si(111)-(3×2) and (2×1) surfaces have been investigated by angle-resolved photoelectron spectroscopy. On the (3×2) surface, we identify six surface states in the gap and a pocket of the bulk band projection. Among the five surface states observed in the bulk band gap, the dispersions of three of them agree well with those of the surface states of monovalent atom adsorbed Si(111)-(3×1) surfaces. The dispersions of the two other surface states observed in the band gap agree well with those observed on the Ca/Si(111)-(3×2) surface, which has basically the same structure as that of monovalent atom adsorbed Si(111)-(3×1) surfaces. Taking these results into account, we conclude that the five surface states observed in the band gap originate from the orbitals of Si atoms that form a honeycomb-chain-channel structure. In the case of the (2×1) surface, two semiconducting states are observed in the bulk band gap. The difference in binding energy of these two states at the $\bar{\Gamma}$ point agrees well with that of the surface states obtained theoretically for a clean Si(111)-(2×1) surface with a Seiwatz structure, and the dispersion of the upper state shows good agreement with the corresponding theoretical surface state. These observations indicate that the two surface states in the band gap originate from Si atoms that form a Seiwatz chain. The present results support the structures of the Eu/Si(111)-(3×2) and (2×1) surfaces proposed in the literature.

DOI: [10.1103/PhysRevB.72.045310](https://doi.org/10.1103/PhysRevB.72.045310)

PACS number(s): 73.20.At, 79.60.-i, 61.14.Hg, 68.35.-p

I. INTRODUCTION

During the past 10 years, one-dimensional (1D) superstructures, which are formed on semiconductor surfaces by the adsorption of metal atoms, have attracted much attention due to the possibility of observing various exotic physical phenomena, such as formations of non-Fermi-liquid like ground states, Peierls-type phase transitions, or order-disorder transitions.¹⁻⁶ These observations led to a profound interest in measuring the electronic structures of 1D and quasi-1D reconstructions induced by the adsorption of rare-earth metals (REM's) on a Si(111) surface.

Several 1D and quasi-1D reconstructions have been reported to be induced by the adsorption of Eu, Yb, and Sm on a Si(111) surface.⁷⁻¹² Of these REM's, Eu has been reported to form a quasi-1D (3×2) reconstruction at a coverage of 1/6 ML, and a series of 1D [(n×1); n=5, 7, and 9] reconstructions at higher coverages culminating in a (2×1) phase at 0.5 ML.¹⁰⁻¹² The lowest coverage (3×2) phase has been proposed to have the same geometric structure as that of alkaline-earth metal (AEM) induced Si(111)-(3×2) surfaces (Refs. 13-20), i.e., the structure is described by the honeycomb-chain-channel (HCC) model (Refs. 21-23) with an adsorbate coverage of 1/6 ML [Fig. 1(a)].^{11,12} Regarding the geometric structure of the highest coverage (2×1) phase, it has been proposed to be the same as that of the Ca/Si(111)-(2×1) surface (Refs. 16, 19, and 24-26), i.e., the Seiwatz structure (Ref. 27) with an adsorbate coverage of 0.5 ML [Fig. 1(b)].¹² The intermediate phases [the (5×1), (7×1), and (9×1) phases] are considered as combinations of the HCC and Seiwatz structures.¹² However, although these reconstructions may show interesting physical phenomena, there is no study on their surface electronic structures so far. Since the structures of the intermediate

phases are proposed to be a combination of the (3×2) and (2×1) phases, an understanding of the surface electronic structures of these two end phases is required in order to comprehend the electronic properties of the Eu induced 1D and quasi-1D reconstructions on a Si(111) surface. Moreover, no strong evidence has been reported regarding the atomic structures of the (3×2) and the (2×1) phases, and the determination of the surface electronic structures of these phases is thus an important input to the structure determination.

In this paper, we present detailed angle-resolved photoelectron spectroscopy (ARPES) measurements performed along the $[\bar{1}10]$ and the $[11\bar{2}]$ directions of the Eu/Si(111)-(3×2) and (2×1) surfaces, i.e., directions parallel and perpendicular to the Eu chains as shown in Fig. 1. Six surface states were observed in the gap and a pocket of the bulk band projection on the (3×2) surface. Among the five surface states in the bulk band gap, the dispersions of three of them follow a (3×1) periodicity instead of the (3×2) periodicity observed in low-energy electron diffraction (LEED). The good agreement between the dispersions of these three states and those of the three surface states of monovalent atom adsorbed (3×1) HCC surfaces indicates that their origins are the same or quite similar. The dispersions of the two other surface states observed in the band gap agree well with those of two of the surface states of the Ca induced Si(111)-(3×2) HCC surface. These results indicate that the five surface states observed in the band gap originate from Si atoms that form a HCC structure. In the case of the (2×1) phase, two semiconducting surface states were observed in the bulk band gap. Of these two states, the dispersion of the upper one agrees well with that of the corresponding surface states obtained theoretically for a clean Si(111)-(2×1) surface with a Seiwatz structure, and that obtained

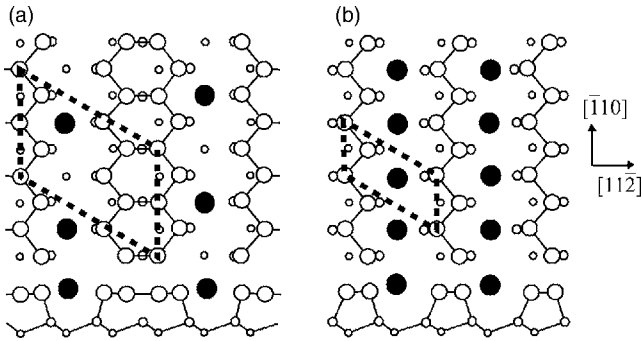


FIG. 1. (a) HCC structure of the Si(111)-(3 \times 2) surface with an adsorbate coverage of 1/6 ML, and (b) Seiwatz structure of the Si(111)-(2 \times 1) surface with an adsorbate coverage of 0.5 ML. Filled circles are metal atoms, which are adsorbed on the T_4 site, and open circles are Si atoms. The dashed lines indicate the unit cell of each surface.

experimentally for the Ca/Si(111)-(2 \times 1) surface. Further, the difference in binding energy of the two observed states agrees well with that of the surface states obtained theoretically at the $\bar{\Gamma}$ point. Taking these results into account, we conclude that the two surface states in the band gap originate from Si atoms that form a Seiwatz chain. The present results strongly support the structures of the Eu/Si(111)-(3 \times 2) and (2 \times 1) surfaces proposed in the literature.

II. EXPERIMENTAL DETAILS

The ARPES measurements were performed at beamline 33 at the MAX-I synchrotron radiation facility in Lund, Sweden. Photoemission spectra were obtained using an angle-resolved photoelectron spectrometer and linearly polarized synchrotron radiation light using three different photon energies ($h\nu=17, 21.2,$ and 35 eV). The total experimental energy resolutions were ~ 45 meV at $h\nu=17$ eV, ~ 50 meV at $h\nu=21.2$ eV, and ~ 100 meV at $h\nu=35$ eV, and the angular resolution was $\pm 2^\circ$. A Si(111) sample (n -type) with a 1.1° miscut towards the $[\bar{1}\bar{1}\bar{2}]$ direction was used as a substrate. To obtain a clean surface, we annealed the sample by direct resistive heating following the procedure described in Refs. 28 and 29. After the annealing, a sharp (7 \times 7) LEED pattern was observed, and neither the valence-band spectra nor the Si $2p$ core-level spectra showed any indication of contamination. The Eu/Si(111)-(3 \times 2) and (2 \times 1) surfaces were prepared by depositing Eu onto a clean Si(111)-(7 \times 7) surface at a substrate temperature of ~ 1080 K. The base pressure was below 8×10^{-11} Torr during the measurements, and below 7×10^{-10} Torr during the Eu evaporation.

III. RESULTS AND DISCUSSION

Figure 2(a) shows the LEED pattern of the Eu/Si(111)-(3 \times 2) surface obtained at 300 K with a primary electron energy of 94 eV. Together with the strong $\times 3$ spots, $\times 2$ streaks are clearly observed in the $[11\bar{2}]$ direction. This observation agrees well with the STM studies,^{11,12} in which

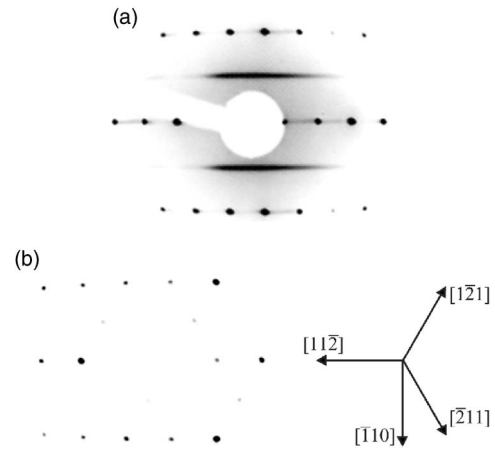


FIG. 2. LEED patterns of (a) the Eu/Si(111)-(3 \times 2) surface obtained at 300 K with a primary electron energy of 94 eV, and (b) the Eu/Si(111)-(2 \times 1) surface obtained at 300 K with a primary electron energy of 124 eV. $\times 2$ streaks are observed together with strong $\times 3$ spots in the $[11\bar{2}]$ direction in (a). Weak $\times 2$ spots are observed in the $[1\bar{2}1]$ and $[\bar{2}11]$ directions in (b).

$\times 2$ modulations were observed along the Eu chains in empty state images. Similar $\times 2$ streaks were reported in the former LEED studies on a Ca/Si(111)-(3 \times 2) surface at 300 K.¹⁷⁻²⁰ In the LEED pattern of the Eu/Si(111)-(2 \times 1) surface [Fig. 2(b)], strong $\times 2$ spots are observed in the $[11\bar{2}]$ direction, whereas only quite weak $\times 2$ spots are observed in the $[1\bar{2}1]$ and $[\bar{2}11]$ directions (the intensity of the $\times 2$ spots in the $[11\bar{2}]$ direction is more than 20 times stronger than in the two other directions). The absence of the $\times 3$ spots and the $\times 2$ streaks in the $[1\bar{2}1]$ and $[\bar{2}11]$ directions in Fig. 2(a) indicates that a very high quality single-domain Eu/Si(111)-(3 \times 2) surface was obtained. The observation of only faint $\times 2$ spots in the $[1\bar{2}1]$ and $[\bar{2}11]$ directions in Fig. 2(b) suggests that the Eu/Si(111)-(2 \times 1) surface is essentially single-domain. These LEED results imply that the ARPES spectra, of both surfaces, can be analyzed without the ambiguity that would have otherwise been caused by contributions from the two other domains.

A. The Eu/Si(111)-(3 \times 2) surface

ARPES spectra of the Eu/Si(111)-(3 \times 2) surface are shown in Fig. 3, together with the Surface Brillouin zones (SBZ's) of the Si(111)-(1 \times 1), (3 \times 1), and (3 \times 2) surfaces [Fig. 3(e)]. (a) and (b) are the spectra measured along the $[\bar{1}\bar{1}0]$ direction, i.e., the direction parallel to the Eu chains, using $h\nu=17$ eV and 21.2 eV, respectively. The spectra in (c) and (d) are measured along the $[11\bar{2}]$ direction, i.e., the direction perpendicular to the Eu chains, using $h\nu=17$ eV and 21.2 eV, respectively. All spectra are normalized to the background intensities at the Fermi position (E_F ; the dashed line in each figure), which was determined by measuring the metallic Fermi edge of a Ta foil fixed on the sample holder. The spectra in the $[11\bar{2}]$ direction were measured using the

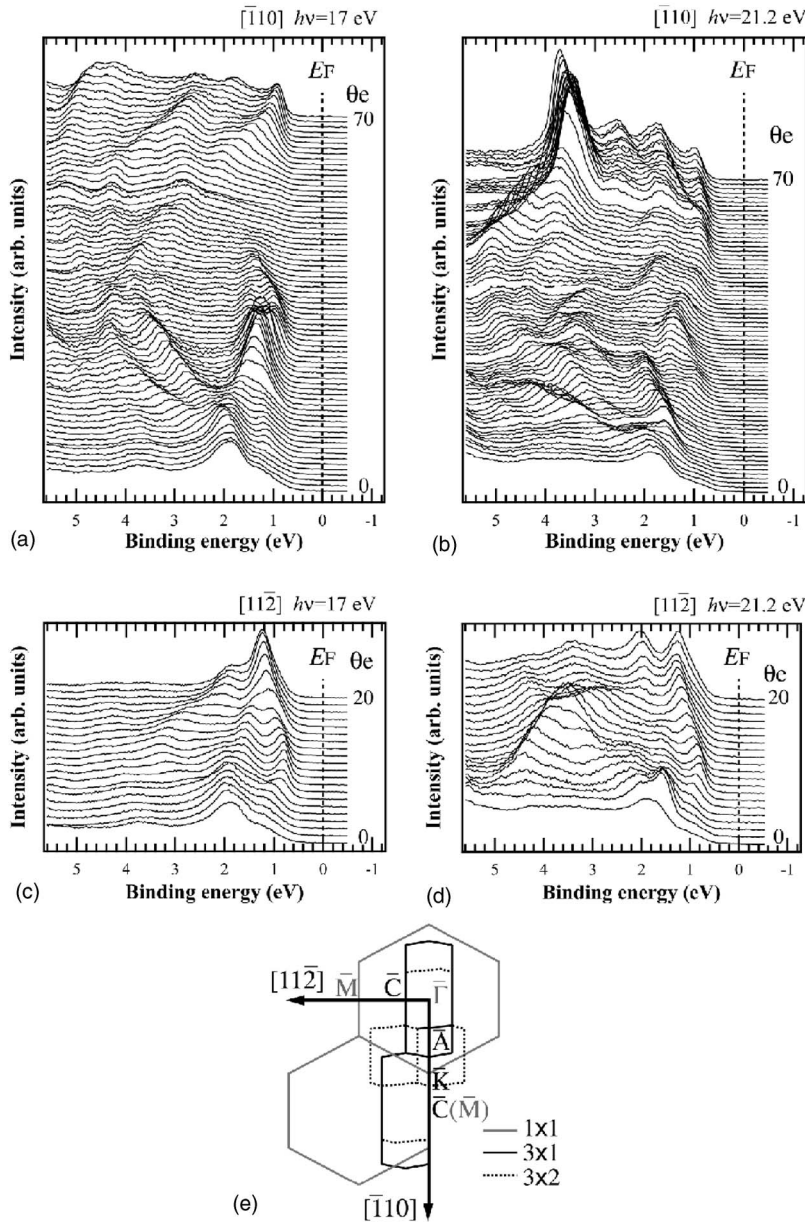


FIG. 3. ARPES spectra of the Eu/Si(111)-(3 \times 2) surface measured along the $[\bar{1}10]$ direction using (a) $h\nu=17$ eV and (b) 21.2 eV, and along the $[11\bar{2}]$ direction using (c) $h\nu=17$ eV and (d) 21.2 eV. The spectra in the $[\bar{1}10]$ direction were obtained using the out-of-plane polarization geometry and the spectra in the $[11\bar{2}]$ direction were measured using the in-plane polarization geometry. (e) SBZ's of the Si(111)-(1 \times 1), (3 \times 1), and (3 \times 2) surfaces. Black letters are the symmetry points of the (3 \times 1) SBZ and the gray letters are those of the (1 \times 1) SBZ in (e).

in-plane polarization geometry (the electric field of photons is parallel to the photoelectron emission plane), and the spectra measured along the $[\bar{1}10]$ direction were obtained using the out-of-plane polarization geometry (the photoelectron emission plane is perpendicular to that of the in-plane polarization geometry). As indicated in Fig. 3(e), the $[\bar{1}10]$ direction corresponds to the $\bar{\Gamma}-\bar{A}-\bar{K}-\bar{C}(\bar{M})$ direction, and the $[11\bar{2}]$ direction corresponds to the $\bar{\Gamma}-\bar{C}$ direction. The symbols \bar{M} and \bar{K} are the symmetry points of the (1 \times 1) SBZ, and the symbols \bar{A} and \bar{C} are the symmetry points of the (3 \times 1) SBZ. The angle-resolved photoelectron spectra were recorded at intervals of 1° from emission angles (θ_e) of 0° to 70° in the $[\bar{1}10]$ direction, and from $\theta_e=0^\circ$ to 20° in the $[11\bar{2}]$ direction. No discernible photoemission intensity is observed from the Fermi level down to a binding energy of 0.4 eV in Figs. 3(a)–3(d). This indicates that the

Eu/Si(111)-(3 \times 2) surface is semiconducting.

The spectra in Fig. 3 show various dispersive features. In order to show the overall band dispersions, the spectra are put into “binding energy– $k_{||}$ ” diagrams, where $k_{||}$ is the momentum parallel to the surface, after being processed by taking the second derivatives of the original ARPES spectra. Figure 4 displays the band dispersions of the Eu/Si(111)-(3 \times 2) surface along the $[\bar{1}10]$ and $[11\bar{2}]$ directions obtained using (a) $h\nu=17$ eV and (b) 21.2 eV. The intensities of the spectral features are approximately represented by the contrast in Fig. 4. Here we notice that the validity of the use of the second derivative of the spectra has been confirmed by comparing the binding energies and contrast in Fig. 4 with binding energies and intensities of the spectral features in Fig. 3 (dark in Fig. 4 corresponds to the highest intensity in the spectra). The heavy dashed lines are the valence band edge and edges of pockets taken from Ref. 30, and the thin dashed lines represent the symmetry points

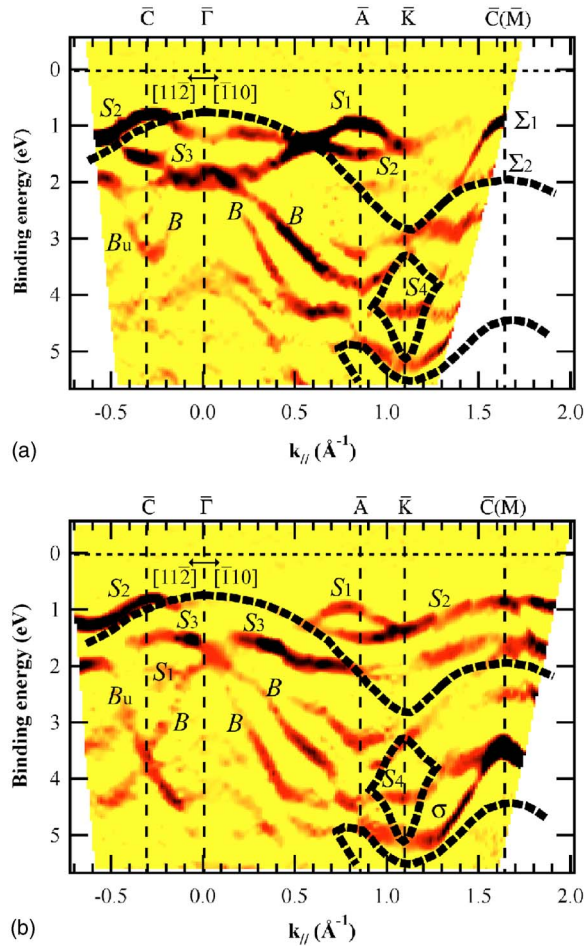


FIG. 4. Band dispersion of the Eu/Si(111)-(3 \times 2) surface measured along the $[\bar{1}10]$ and $[11\bar{2}]$ directions using (a) $h\nu=17$ eV and (b) 21.2 eV. The heavy dashed lines are the valence band edge and edges of pockets taken from Ref. 30, and the thin dashed lines represent the symmetry points indicated at the top of each figure. The contrast represents the second derivatives of the original ARPES spectra shown in Fig. 3.

of the (1 \times 1) and (3 \times 1) SBZ's indicated at the top of each figure. The valence band maximum (VBM) is estimated from the binding energy of the Si 2*p* core level using the relation between $E_{B(\text{VBM})}$, E_F , and $E_{B(\text{Si}2p_{3/2})}$ given in Ref. 31.

Six surface states, denoted as S_1 - S_4 , Σ_1 , and Σ_2 , are identified in the gap and a pocket of the bulk band projection in Fig. 4. Of these six states, S_1 , which is clearly observed in Fig. 4(a), disperses upward from the $\bar{\Gamma}$ point to the \bar{A} point and downward from the \bar{A} point to the \bar{K} point in the $[\bar{1}10]$ direction. Along the $[11\bar{2}]$ direction, S_1 is faintly observed around the \bar{C} point. The dispersion width of S_1 is approximately 1 eV in the $[\bar{1}10]$ direction and less than 0.2 eV in the $[11\bar{2}]$ direction. S_2 has a downward dispersion from the $\bar{\Gamma}$ point to the \bar{A} point and an upward dispersion from the \bar{A} point to the \bar{C} point along the $[\bar{1}10]$ direction, and it disperses upward from the $\bar{\Gamma}$ point to the \bar{C} point and downward from the \bar{C} point to the $\bar{\Gamma}$ point of the second SBZ along the

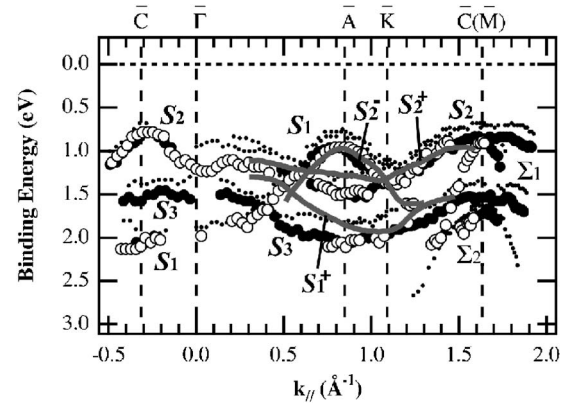


FIG. 5. Surface state dispersions of the Eu/Si(111)-(3 \times 2) surface along the $\bar{\Gamma}$ - \bar{C} and $\bar{\Gamma}$ - \bar{A} - \bar{K} - $\bar{C}(\bar{M})$ directions. The open circles represent the peak and shoulder positions of the ARPES spectra obtained using $h\nu=17$ eV, and the filled ones are those obtained using $h\nu=21.2$ eV. Small dots are the surface states of the Ca/Si(111)-(3 \times 2) surface derived from Ref. 20. Gray solid curves, labeled S_1^+ , S_2^+ , and S_3^+ , are the theoretical surface state dispersions derived from the calculation for the Li/Si(111)-(3 \times 1) surface (Ref. 21).

$[11\bar{2}]$ direction. The S_3 state shows the same dispersion feature as that of S_2 in the $[\bar{1}10]$ direction, but hardly disperses in the $[11\bar{2}]$ direction. The dispersion widths of S_2 and S_3 are approximately 0.7 eV and 0.55 eV in the $[\bar{1}10]$ direction, and approximately 0.4 eV and less than 0.1 eV in the $[11\bar{2}]$ direction, respectively. The dispersion features of the S_1 - S_3 states indicate that these three surface states follow a (3 \times 1) periodicity instead of the (3 \times 2) periodicity observed in LEED [Fig. 2(a)]. Concerning S_4 , Σ_1 , and Σ_2 we cannot discuss their detailed dispersion features since they are only observed in small $k_{||}$ regions.

In addition to the above six surface states, two other states (denoted as B_u and σ) that are not observed on the Si(111)-(7 \times 7) surface, are shown in Fig. 4. Since B_u can be reproduced by folding the B state, this state should result from the folding of a bulk state by a reciprocal lattice vector of the high quality (3 \times 2) surface used in the present study. A state that has the same dispersion features as B_u , and that is assigned to originate from an umklapp process, was also reported on the Ba¹³ and Ca²⁰ adsorbed Si(111)-(3 \times 2) surfaces. The σ state has an upward dispersion from the \bar{K} point to the \bar{M} point, and its binding energy is approximately 5 eV at the \bar{K} point. Since this is roughly the dispersion expected for a direct transition at $h\nu=21.2$ eV,³² the origin of σ might be a direct bulk transition.

In order to discuss the surface electronic structure of the Eu/Si(111)-(3 \times 2) surface, we compare the band dispersions of the five surface states observed in the bulk band gap (the S_1 - S_3 , Σ_1 , and Σ_2 states) with the dispersions of the surface states obtained theoretically for the Li/Si(111)-(3 \times 1) surface,²¹ and those obtained experimentally for the Ca/Si(111)-(3 \times 2) surface.²⁰ The open circles in Fig. 5 represent the peak and shoulder positions of the ARPES

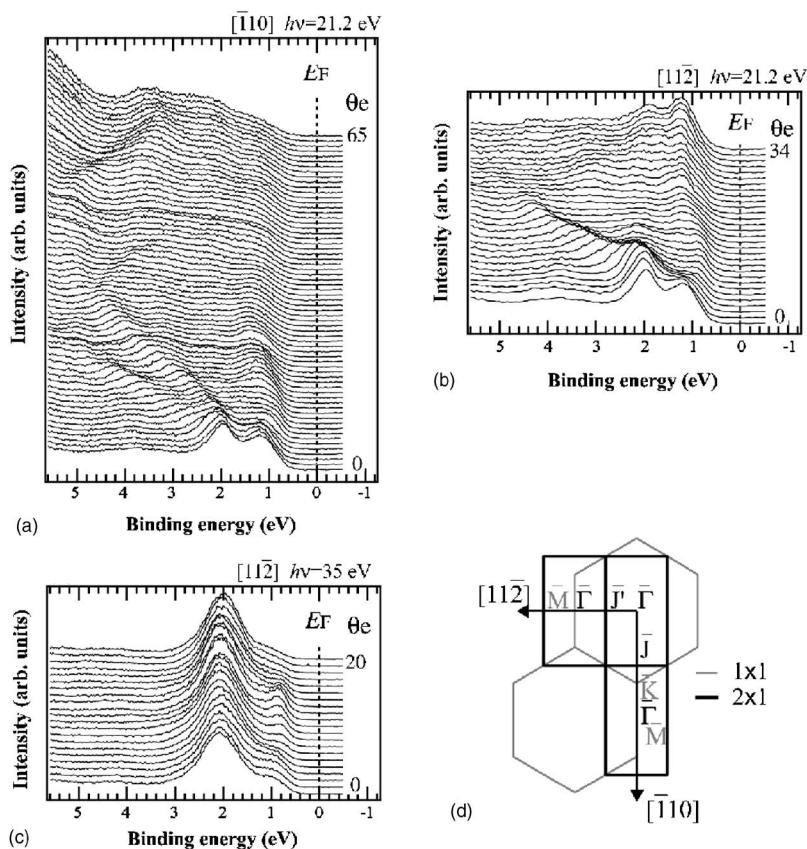


FIG. 6. ARPES spectra of the Eu/Si(111)-(2 × 1) surface measured (a) along the $[\bar{1}10]$ direction using $h\nu=21.2$ eV, and along the $[11\bar{2}]$ direction using (b) $h\nu=21.2$ eV and (c) 35 eV. The spectra in the $[\bar{1}10]$ direction were obtained using the out-of-plane polarization geometry and the spectra in the $[11\bar{2}]$ direction were measured using the in-plane polarization geometry. (d) SBZ's of the Si(111)-(1 × 1) and (2 × 1) surfaces. Black letters are the symmetry points of the (2 × 1) SBZ and the gray letters are those of the (1 × 1) SBZ in (d).

spectra obtained using $h\nu=17$ eV, and the filled ones are those obtained using $h\nu=21.2$ eV. The gray solid lines, which are labeled S_1^+ , S_2^+ , and S_2^- , are the dispersions of the surface states derived from the theoretical calculation, and the small dots are the surface states of Ca/Si(111)-(3 × 2). As shown in Fig. 5, the dispersion features of S_1 - S_3 agree well with those of the calculated states. The relative binding energies of S_1 and S_2 show good agreement with those of S_2^+ and S_2^- and the relative binding energy of S_3 agrees well with that of S_1^+ at k_{\parallel} larger than 0.9 \AA^{-1} . Further, the photoemission cross sections of S_1 - S_3 coincide with those of S_1^+ , S_2^+ , and S_2^- , i.e., S_1 and S_2 have quite small photoemission cross sections in the measurement using the in-plane geometry along the $[\bar{1}10]$ direction, while the cross sections of S_2 , S_3 , S_1^+ , and S_2^+ do not have such dependence. Both the dispersion features and binding energies of S_1 - S_3 also agree well with those of the surface states of the Ca/Si(111)-(3 × 2) surface. Taking these good agreements into account, we conclude that the origins of S_1 - S_3 are the same or quite similar to those of the Li/Si(111)-(3 × 1) and Ca/Si(111)-(3 × 2) surfaces. This conclusion supports that the basic atomic structure of the Eu/Si(111)-(3 × 2) surface is HCC [Fig. 1(a)].

Regarding the origins of the surface states, the above conclusion indicates that the S_1 and S_2 states originate from the orbitals of Si atoms that face the channel, and that the origin of S_3 is the π -bond state formed by two Si atoms that are contained in the honeycomb and do not face the channel. These assignments are in accordance with the origins of S_1^+ , S_2^+ , and S_2^- reported in Ref. 21. [The binding energy of S_3

is different from that of S_1^+ at k_{\parallel} smaller than 0.9 \AA^{-1} , but since it shows good agreement with one of the surface states of the Ca/Si(111)-(3 × 2) surface, and because this small difference should not affect the conclusion on the origin of the S_3 state, we do not discuss this difference in detail.] Surface states, whose binding energies are the same as that of S_4 , were observed for the Na,³³ K,³⁴ Ag,^{6,35} and Ca (Ref. 20) adsorbed Si(111)-(3 × 1) and (3 × 2) surfaces. Taking into account that the basic atomic structure of all these (3 × 1) and (3 × 2) surfaces is HCC, these observations suggest that S_4 is a surface state that originates from orbitals of Si atoms that form the HCC structure. As shown in Fig. 5, surface states, whose dispersion features and binding energies are similar to those of Σ_1 and Σ_2 , were observed in the former study performed on the Ca/Si(111)-(3 × 2) surface.²⁰ Since these states were not observed on alkali-metal atom induced Si(111)-(3 × 1) surfaces,^{6,33,34,36} they should be surface states peculiar to the (3 × 2) periodic HCC surfaces. Further, taking the adsorbate coverage into account, the agreements in the number of surface states and their dispersions indicate the donation of two electrons per (3 × 2) unit cell, and thus the ionic interaction between Eu and Si atoms. These indications support the report that the HCC reconstruction is stabilized by the donation of one electron per (3 × 1) unit cell,¹⁴ and also suggest the valence state of the adsorbate to be Eu^{2+} .

As mentioned above, the LEED pattern of the Eu/Si(111)-(3 × 2) surface shown in Fig. 2(a) is similar to that of the Ca/Si(111)-(3 × 2) surface observed at 300 K. However, in contrast to the Ca/Si(111)-(3 × 2) surface, on

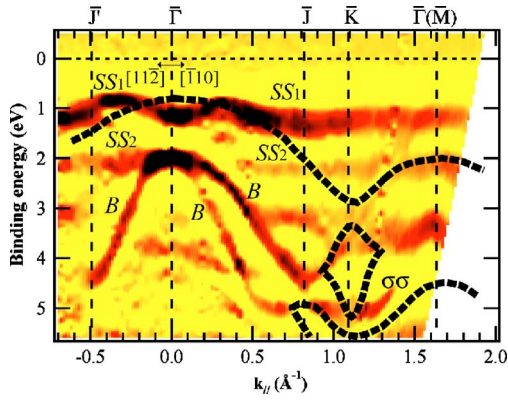


FIG. 7. Band dispersion of the Eu/Si(111)-(2 \times 1) surface measured along the $[11\bar{2}]$ and $[\bar{1}10]$ directions using $h\nu=21.2$ eV. The heavy dashed lines are the valence band edge and edges of pockets taken from Ref. 30, and the thin dashed lines represent the symmetry points indicated at the top of each figure.

which half-order spots of the (3 \times 2) reconstruction were observed at 100 K,^{16,20} only the $\times 2$ streaks were observed and no half-order spot was observed at 100 K on the Eu/Si(111)-(3 \times 2) surface. Since the $\times 2$ streaks observed on the Ca/Si(111)-(3 \times 2) surface at 300 K are reported to result from the thermally induced diffusion of the Ca atoms along the chain,²⁰ this difference might result from the different Debye temperatures of the two surfaces.

B. The Eu/Si(111)-(2 \times 1) surface

In Fig. 6, we show the ARPES spectra of the Eu/Si(111)-(2 \times 1) surface measured (a) along the $[\bar{1}10]$ direction using $h\nu=21.2$ eV and along the $[11\bar{2}]$ direction using (b) $h\nu=21.2$ eV and (c) 35 eV, together with (d) the SBZ's of the Si(111)-(1 \times 1) and (2 \times 1) surfaces. The spectra, which are normalized to the background intensities at E_F , were measured using the same geometries as those used on the Eu/Si(111)-(3 \times 2) surface along each direction. As indicated in Fig. 6(d), the $[\bar{1}10]$ direction corresponds to the $\bar{\Gamma}$ - \bar{J} - \bar{K} - $\bar{\Gamma}(\bar{M})$ direction, and the $[11\bar{2}]$ direction corresponds to the $\bar{\Gamma}$ - \bar{J}' - $\bar{\Gamma}(\bar{M})$ direction. The symbols \bar{J} and \bar{J}' are the symmetry points of the (2 \times 1) SBZ. The angle-resolved photoelectron spectra were recorded at every 1 $^\circ$ emission angle in each direction. By comparing the spectra in Figs. 6(b) and 6(c), we notice that the cross section of the state with a binding energy of approximately 1 eV is larger using $h\nu=21.2$ eV, and the cross section of the state at approximately 2 eV is larger using $h\nu=35$ eV. Since none of these states crosses the Fermi level and no other state is observed at a binding energy lower than these states, we conclude that the electronic structure of the Eu/Si(111)-(2 \times 1) surface is semiconducting in similarity with the (3 \times 2) surface.

Figure 7 displays the band dispersions of the Eu/Si(111)-(2 \times 1) surface along the $[\bar{1}10]$ and $[11\bar{2}]$ directions obtained using $h\nu=21.2$ eV. The heavy dashed lines are the valence band edge and edges of pockets taken from

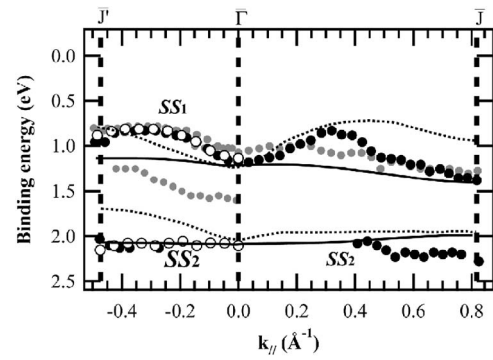


FIG. 8. Surface state dispersions of the Eu/Si(111)-(2 \times 1) surface along the \bar{J}' - $\bar{\Gamma}$ - \bar{J} symmetry lines. The filled circles represent the peak and shoulder positions of the ARPES spectra obtained using $h\nu=21.2$ eV, and the open ones are those obtained using $h\nu=35$ eV. Gray circles are the surface states of the Ca/Si(111)-(2 \times 1) surface derived from Ref. 26. Solid (Ref. 37) and dashed (Ref. 38) curves are the theoretical surface state dispersions derived from calculation for the Si(111)-(2 \times 1) clean surface with Seiwatz structures.

Ref. 30, and the thin dashed lines represent the symmetry points of the (1 \times 1) and (2 \times 1) SBZ's indicated at the top of each figure. The intensities of the spectral features are approximately represented by the brightness of the gray-scale as in Fig. 4. Two surface states, denoted as SS_1 and SS_2 , are clearly observed in the gap of the bulk band projection in Fig. 7. The SS_1 state disperses first upward and then downward from the $\bar{\Gamma}$ point to the \bar{J} point along the $[\bar{1}10]$ direction. Along the $[11\bar{2}]$ direction, SS_1 shows an upward dispersion from the $\bar{\Gamma}$ point to the \bar{J}' point, and a downward dispersion from the \bar{J}' point to the $\bar{\Gamma}$ point of the second SBZ. The dispersion width of the SS_1 state is approximately 0.55 eV in the $[\bar{1}10]$ direction, and it is approximately 0.35 eV in the $[11\bar{2}]$ direction. The dispersion features of the SS_1 state indicate that this surface state follows a (2 \times 1) periodicity. In contrast to the SS_1 state, SS_2 hardly disperses in either of the two directions. Besides these two surface states, another state (denoted as $\sigma\sigma$), is shown in Fig. 7. Since both the dispersion feature and binding energy of this state show good agreements with those of the $\sigma\sigma$ state observed on the Eu/Si(111)-(3 \times 2) surface, the origin of $\sigma\sigma$ might be a direct bulk transition as well.

The SS_1 and SS_2 bands are compared with the surface bands obtained experimentally for the Ca/Si(111)-(2 \times 1) surface²⁶ and with those obtained by the theoretical calculations performed for the Si(111)-(2 \times 1) clean surface with Seiwatz structure^{37,38} in Fig. 8. Here we notice that although the structure of the Si(111)-(2 \times 1) surface is called the three-bond scission (TBS) model in Refs. 37 and 38, we use the name Seiwatz in the present paper since first the structures of the two models are basically the same, and second the name Seiwatz was used in the literature on the metal atoms induced Si(111)-(2 \times 1) surfaces. Further, since the interaction between Eu and Si atoms would be ionic on a Eu/Si(111)-(2 \times 1) surface likewise the interaction on a

Eu/Si(111)-(3×2) surface, we compare the SS_1 and SS_2 states with the two surface states of the Si(111)-(2×1) clean surface that are originally situated just above and just below the Fermi level.

The filled circles in Fig. 8 represent the peak and shoulder positions of the ARPES spectra obtained using $h\nu=21.2$ eV, and the open ones are those obtained using $h\nu=35$ eV. The gray circles are the surface states of the Ca/Si(111)-(2×1) surface,²⁶ and the solid lines are the dispersions of the surface states derived from the theoretical calculations in Ref. 37, and the dashed lines are those derived from Ref. 38. The binding energies of the calculated surface states are shifted to fit the upper calculated surface states to the binding energy of the SS_1 state at the $\bar{\Gamma}$ point. Concerning the solid lines, the dispersion widths of the two calculated surface states and the gap between them were reduced by a factor of 8 from their original values (the factor was chosen to fit the calculated gap and the gap between SS_1 and SS_2) by considering that the dispersion widths and the band gap reported in Ref. 37 was stated to be overestimated.³⁸

The dispersion features of the two surface states are similar in both calculations, though they are performed using different methods and different magnitude of buckling for Si atoms forming Seiwatz chains. That is, the upper surface state disperses first slightly upward and then downward from the $\bar{\Gamma}$ point to the \bar{J} point and upward from the $\bar{\Gamma}$ point to the \bar{J}' point, and the lower surface state disperses upward in both the $\bar{\Gamma}-\bar{J}$ and the $\bar{\Gamma}-\bar{J}'$ directions. Compared with the dispersions of the surface states of the Si(111)-(2×1) clean surface with the Seiwatz structure, those of the Si(111)-(2×1) clean surface with other structures are different. The corresponding two surface states disperse downward in the $\bar{\Gamma}-\bar{J}'$ direction with a Pandey π -bonded chain structure,³⁸⁻⁴⁰ and the upper surface state has only a continuative downward dispersion in the $\bar{\Gamma}-\bar{J}$ direction with a buckling structure.^{37,41,42} This indicates that the dispersion feature of the SS_1 state is in agreement with that of one of the surface states of a clean surface with a Seiwatz structure, but not with those of clean surfaces with other structures. The dispersion feature of the SS_1 state also agrees well with the upper surface state of the Ca/Si(111)-(2×1) surface.

In contrast to the SS_1 state, the dispersion feature of SS_2 does not agree with that of the calculated lower surface states (dashed line) shown in Fig. 8 though the difference in binding energy between SS_1 and SS_2 shows a good agreement with the difference in binding energy between the two surface states predicted from Ref. 38 at the $\bar{\Gamma}$ point. This disagreement might result from the presence of another state whose binding energy is close to that of SS_2 . In fact, the broader width of the spectral feature for SS_2 in comparison with that of the SS_1 state [this is obvious by comparing the spectra measured at $\theta_e=34^\circ$ in Fig. 6(b) and at around $\theta_e=10^\circ$ in Fig. 6(c)], indicates the presence of another state at a binding energy of 2 eV or so. Therefore, since an ionic interaction hardly affects the dispersion features of surface states, we conclude that the SS_1 state and probably a part of the SS_2 originate from orbitals of Si atoms that form a Seiwatz structure. Moreover, the observation of the semicon-

ducting SS_1 state suggests that the lowest unoccupied surface state of the Si(111)-(2×1) clean surface with a Seiwatz structure is fully occupied by the donation of two electrons per (2×1) unit cell. The presence of a Seiwatz structure and the number of electrons per unit cell support the surface structure of the Eu/Si(111)-(2×1) surface proposed in the literature,¹² and also suggest that the valence state of the adsorbate is Eu^{2+} as well as the (3×2) surface. Further, taking into account that a difference in magnitude of buckling might cause different dispersion widths and that the dispersion width of the SS_1 state is different from that of the corresponding surface state of the Ca/Si(111)-(2×1) surface, we propose that the bucklings for Si atoms forming Seiwatz chains are different on these two metal induced (2×1) surfaces.

IV. CONCLUSION

In conclusion, we have studied the electronic structures of the Eu/Si(111)-(3×2) and (2×1) surfaces along the $[\bar{1}10]$ and the $[11\bar{2}]$ directions using ARPES. On the (3×2) surface, six states were observed in the gap and a pocket of the bulk band projection. Of the five surface states observed in the bulk band gap, the dispersions of S_1 - S_3 follow a (3×1) periodicity instead of the (3×2) periodicity observed in LEED. Further, their dispersions show good agreement with those of the surface states of monovalent atom adsorbed (3×1) HCC surfaces in the $[\bar{1}10]$ direction. This indicates that S_1 - S_3 are surface states whose origins are the same or quite similar to those of the Si(111)-(3×1) surfaces. The two other states observed in the band gap, the Σ_1 and Σ_2 states, were not observed on monovalent atom adsorbed (3×1) HCC surfaces. Since their dispersions agree well with the surface states of Ca/Si(111)-(3×2), we conclude that they are surface states peculiar to the (3×2) periodic HCC surfaces. Regarding the (2×1) phase, two semiconducting surface states (SS_1 and SS_2) were observed in the bulk band gap. Of these two states, the dispersion of SS_1 completely follows a (2×1) periodicity. The SS_1 state disperses slightly upward and then downward from the $\bar{\Gamma}$ point to the \bar{J} point, and upward from the $\bar{\Gamma}$ point to the \bar{J}' point. This dispersion feature agrees well with the dispersion of the surface state obtained theoretically for a clean Si(111)-(2×1) surface with a Seiwatz structure and experimentally for the Ca/Si(111)-(2×1) surface. The difference in binding energy of the SS_1 and SS_2 states agrees well with that of the surface states obtained theoretically at the $\bar{\Gamma}$ point. These good agreements indicate that the SS_1 state and probably a part of the SS_2 originate from orbitals of Si atoms that form a Seiwatz structure. The above conclusions give strong evidence that the Eu/Si(111)-(3×2) surface is formed by a HCC structure with a 1/6 ML coverage and the Eu/Si(111)-(2×1) surface is formed by a Seiwatz structure with a 0.5 ML coverage as proposed in the literature. Moreover, the close resemblances between the electronic structures of the Eu induced reconstructions and the Ca induced ones suggest that the valence state of the adsorbate is Eu^{2+}

on both the Eu/Si(111)-(3×2) and (2×1) surfaces.

ACKNOWLEDGMENTS

Experimental support from Dr. T. Balasubramanian, Dr. J. He, and the MAX-lab staff, and suggestions on the sample

preparation from Dr. K. Shimada are gratefully acknowledged. This work was financially supported by the Swedish Research Council and the Ministry of Education, Culture, Sports, Science and Technology of the Japanese Government. K.S. was partially supported by the MEXT 21st Century COE program “Exploring New Science by Bridging Particle-Matter Hierarchy.”

*Electronic address: sakamoto@surface.phys.tohoku.ac.jp

- ¹P. Segovia, D. Purdie, M. Hengsberger, and Y. Baer, *Nature (London)* **402**, 504 (1999).
- ²H. W. Yeom, S. Takeda, E. Rotenberg, I. Matsuda, K. Horikoshi, J. Schaefer, C. M. Lee, S. D. Kevan, T. Ohta, T. Nagao, and S. Hasegawa, *Phys. Rev. Lett.* **82**, 4898 (1999).
- ³O. Gallus, Th. Pillo, M. Hengsberger, P. Segovia, and Y. Baer, *Eur. Phys. J. B* **20**, 313 (2001).
- ⁴R. Losio, K. N. Altmann, A. Kirakosian, J. L. Lin, D. Y. Petrovykh, and F. J. Himpsel, *Phys. Rev. Lett.* **86**, 4632 (2001).
- ⁵I. K. Robinson, P. A. Bennett, and F. J. Himpsel, *Phys. Rev. Lett.* **88**, 096104 (2002).
- ⁶K. Sakamoto, H. Ashima, H. M. Zhang, and R. I. G. Uhrberg, *Phys. Rev. B* **65**, 045305 (2002).
- ⁷C. Wigren, J. N. Andersen, R. Nyholm, M. Göthelid, M. Hammar, C. Törnevik, and U. O. Karlsson, *Phys. Rev. B* **48**, 11 014 (1993).
- ⁸C. Wigren, J. N. Andersen, R. Nyholm, U. O. Karlsson, J. Nogami, A. A. Baski, and C. F. Quate, *Phys. Rev. B* **47**, 9663 (1993).
- ⁹M. Kuzmin, P. Laukkanen, R. E. Perälä, and I. J. Väyrynen, *Surf. Sci.* **515**, 471 (2002).
- ¹⁰T. V. Krachino, M. V. Kuz'min, M. V. Loginov, and M. A. Mitsev, *Appl. Surf. Sci.* **182**, 115 (2001).
- ¹¹M. Kuzmin, R.-L. Vaara, P. Laukkanen, R. E. Perälä, and I. J. Väyrynen, *Surf. Sci.* **538**, 124 (2003).
- ¹²R.-L. Vaara, M. Kuzmin, P. Laukkanen, R. E. Perälä, and I. J. Väyrynen, *Appl. Surf. Sci.* **220**, 327 (2003).
- ¹³T. Okuda, H. Ashima, H. Takeda, K. S. An, A. Harasawa, and T. Kinoshita, *Phys. Rev. B* **64**, 165312 (2001).
- ¹⁴G. Lee, S. Hong, H. Kim, D. Shin, J.-Y. Koo, H.-I. Lee, and D.-W. Moon, *Phys. Rev. Lett.* **87**, 056104 (2001).
- ¹⁵J. Schäfer, S. C. Erwin, M. Hansmann, Z. Song, E. Rotenberg, S. D. Kevan, C. S. Hellberg, and K. Horn, *Phys. Rev. B* **67**, 085411 (2002).
- ¹⁶K. Sakamoto, W. Takeyama, H. M. Zhang, and R. I. G. Uhrberg, *Phys. Rev. B* **66**, 165319 (2002).
- ¹⁷D. Y. Petrovykh, K. N. Altmann, J.-L. Lin, F. J. Himpsel, and F. M. Leibsle, *Surf. Sci.* **512**, 269 (2002).
- ¹⁸O. Gallus, Th. Pillo, P. Starowicz, and Y. Baer, *Europhys. Lett.* **60**, 903 (2002).
- ¹⁹Y. K. Kim, J. W. Kim, H. S. Lee, Y. J. Kim, and H. W. Yeom, *Phys. Rev. B* **68**, 245312 (2003).
- ²⁰K. Sakamoto, H. M. Zhang, and R. I. G. Uhrberg, *Phys. Rev. B* **69**, 125321 (2004).
- ²¹S. C. Erwin and H. H. Weitering, *Phys. Rev. Lett.* **81**, 2296 (1998).
- ²²L. Lottermoser, E. Landemark, D.-M. Smilgies, M. Nielsen, R. Feidenhans'l, G. Falkenberg, R. L. Johnson, M. Gierer, A. P. Seitsonen, H. Kleine, H. Bludau, H. Over, S. K. Kim, and F. Jona, *Phys. Rev. Lett.* **80**, 3980 (1998).
- ²³M.-H. Kang, J.-H. Kang, and S. Jeong, *Phys. Rev. B* **58**, R13 359 (1998).
- ²⁴A. A. Baski, S. C. Erwin, M. S. Turner, K. M. Jones, J. W. Dickinson, and J. A. Carlisle, *Surf. Sci.* **476**, 22 (2001).
- ²⁵T. Sekiguchi, F. Shimokoshi, T. Nagao, and S. Hasegawa, *Surf. Sci.* **493**, 148 (2001).
- ²⁶K. Sakamoto, H. M. Zhang, and R. I. G. Uhrberg, *Phys. Rev. B* **68**, 245316 (2003).
- ²⁷R. Seiwatz, *Surf. Sci.* **2**, 473 (1964).
- ²⁸J. Viernow, J.-L. Lin, D. Y. Petrovykh, F. M. Leibsle, F. K. Men, and F. J. Himpsel, *Appl. Phys. Lett.* **72**, 948 (1998).
- ²⁹J.-L. Lin, D. Y. Petrovykh, J. Viernow, F. K. Men, D. J. Seo, and F. J. Himpsel, *J. Appl. Phys.* **84**, 255 (1998).
- ³⁰J. Ihm, M. L. Cohen, and J. R. Chelikowsky, *Phys. Rev. B* **22**, 4610 (1980).
- ³¹F. J. Himpsel, G. Hollinger, and R. A. Pollak, *Phys. Rev. B* **28**, 7014 (1983).
- ³²R. I. G. Uhrberg, G. V. Hansson, J. M. Nicholls, P. E. S. Persson, and S. A. Flodström, *Phys. Rev. B* **31**, 3805 (1985), and references therein.
- ³³T. Okuda, K. Sakamoto, H. Nishimoto, H. Daimon, S. Suga, T. Kinoshita, and A. Kakizaki, *Phys. Rev. B* **55**, 6762 (1997).
- ³⁴K. Sakamoto, T. Okuda, H. Nishimoto, H. Daimon, S. Suga, T. Kinoshita, and A. Kakizaki, *Phys. Rev. B* **50**, 1725 (1994).
- ³⁵M. Gurnett, J. B. Gustafsson, K. O. Magnusson, S. M. Widstrand, and L. S. O. Johansson, *Phys. Rev. B* **66**, 161101(R) (2002).
- ³⁶H. H. Weitering, X. Shi, and S. C. Erwin, *Phys. Rev. B* **54**, 10585 (1996).
- ³⁷B. Chen and D. Haneman, *Phys. Rev. B* **51**, 4258 (1995).
- ³⁸S.-H. Lee and M.-H. Kang, *Phys. Rev. B* **54**, 1482 (1996).
- ³⁹K. C. Pandey, *Phys. Rev. Lett.* **47**, 1913 (1981).
- ⁴⁰J. E. Northrup and M. L. Cohen, *Phys. Rev. Lett.* **49**, 1349 (1982).
- ⁴¹D. Vanderbilt and S. G. Louie, *J. Vac. Sci. Technol. B* **1**(3), 723 (1983).
- ⁴²R. Del Sole and D. J. Chadi, *Phys. Rev. B* **24**, 7431 (1981).